The structure of the outer membrane protein OmpX from *Escherichia coli* reveals possible mechanisms of virulence

Joachim Vogt and Georg E Schulz*

Background: The integral outer membrane protein X (OmpX) from *Escherichia coli* belongs to a family of highly conserved bacterial proteins that promote bacterial adhesion to and entry into mammalian cells. Moreover, these proteins have a role in the resistance against attack by the human complement system. Here we present the first crystal structure of a member of this family.

Results: The crystal structure of OmpX from *E. coli* was determined at 1.9 Å resolution using multiple isomorphous replacement. OmpX consists of an eight-stranded antiparallel all-next-neighbor β barrel. The structure shows two girdles of aromatic amino acid residues and a ribbon of nonpolar residues that attach to the membrane interior. The core of the barrel consists of an extended hydrogen-bonding network of highly conserved residues. OmpX thus resembles an inverse micelle. The structure explains the dramatically improved crystal quality of OmpX containing the mutation His100→Asn, which made the X-ray analysis possible. The coordination spheres of two bound platinum ions are described.

Conclusions: The OmpX structure shows that within a family of virulence-related membrane proteins, the membrane-spanning part of the protein is much better conserved than the extracellular loops. Moreover, these loops form a protruding β sheet, the edge of which presumably binds to external proteins. It is suggested that this type of binding promotes cell adhesion and invasion and helps defend against the complement system. Although OmpX has the same β-sheet topology as the structurally related outer membrane protein A (OmpA), their barrels differ with respect to the shear numbers and internal hydrogen-bonding networks.

Address: Institut für Organische Chemie und Biochemie, Albert-Ludwigs-Universität, Albertstraβe 21, D-79104 Freiburg im Breisgau, Germany.

*Corresponding author.
E-mail: schulz@bio.chemie.uni-freiburg.de

Key words: bacterial defense system, β-barrel, coordination sphere, integral membrane protein, OmpX, platinum, X-ray analysis

Received: 18 May 1999
Revisions requested: 22 June 1999
Revisions received: 5 July 1999
Accepted: 6 July 1999

Published: 1 October 1999

Structure October 1999, 7:1301–1309
http://biomednet.com/elecref/0969212600701301

0969-2126/99/$ – see front matter

Introduction

Bacterial pathogens have evolved numerous strategies for neutralizing host defense mechanisms, among which are adhesion to host cells and entry into them. The sites of interaction between bacteria and host reside in the bacterial outer membrane. Another way of resisting host defenses is to interfere with the complement system. Such resistance is characteristic of all Gram-negative bacteria that cause septicemia [1] and is associated with a family of outer membrane proteins that includes OmpX from *Escherichia coli* [2]. Outer membrane proteins homologous with OmpX have been characterized from *Enterobacter cloacae* (OmpX), *Klebsiella pneumoniae* (OmpK17), *Salmonella typhimurium* (PagC and Rck), *Yersinia enterocolitica* (Ail) and bacteriophage λ (Lom) [2].

There is a causal relationship between the high expression of OmpX in *E. cloacae* and invasiveness into rabbit ileal tissue [3]. Moreover, the overproduction of *E. cloacae* OmpX in *E. coli* (or in *E. cloacae*) is known to decrease the amounts of the porins OmpF and OmpC (or the respective porins in *E. cloacae*), giving rise to resistance to β-lactams [4]. OmpK17 from *K. pneumoniae* confers resistance against the bacteriocin 28b from *Serratia marcescens* [5]. PagC is required by *S. typhimurium* for survival in macrophages and for virulence in mice [6]. Mechanistic studies with Rck from a virulence plasmid of *S. typhimurium* suggested that Rck inhibits the functional assembly of the membrane-attack complex of the complement system [7]. Ail promotes adhesion to and invasion of tissue culture cells and is involved in resistance against the host defense system [8,9]. Lom is an outer membrane protein encoded by bacteriophage λ and expressed during λ lysogeny; it promotes the adhesion of *E. coli* to human cells, thus increasing the competitiveness of λ-infected bacteria [10,11]. Here we present the first high-resolution structure of a member of this defense-oriented family of integral membrane proteins, revealing a new type of β barrel and suggesting an explanation for virulence.

Results and discussion

Structure analysis

All crystals analyzed were from the recombinant mutant His100 → Asn (H100N), which shows greatly improved crystal properties compared with wild type. The protein was expressed in inclusion bodies, (re)natured and crystallized

as described previously [12]. An attempt to solve the structure by molecular replacement with OmpA [13] failed, and we had to use multiple isomorphous replacement (MIR). A native data set and two heavy-atom derivative data sets were collected on a rotating anode at room temperature (Table 1). The heavy-atom positions were determined by difference-Patterson and difference-Fourier methods. After the refinement of the heavy-atom positions and after several cycles of density modification, the electron-density map obtained at 3.3 Å resolution was interpretable and could be used for model building. The model based on the initial phases contained 128 of the 148 residues (M_r 16,383 for the wild type). In a first round of refinement, the R factor dropped to 33.5% (the R_{free} was 37.3%).

By chance the best data set (Cryo-Pt) was obtained from a K_2PtCl_4-soaked crystal using synchrotron radiation at cryogenic temperatures (Table 2). The initial model was therefore refined using data set Cryo-Pt. The resulting model contained all 148 amino acids. Further continuous densities were interpreted as one molecule of n-octyltetraoxyethylene (C_8E_4, the detergent used for crystallization) and two molecules of the cryoprotectant glycerol. None of them is at a crystal packing contact. Using the program ARPP [14], 73 water molecules were introduced. The final data are given in Table 2. The chain fold is depicted in Figure 1.

Two regions of the electron density were interpreted as platinum atoms, each with two chloride ions in the coordination sphere. One $PtCl_2$ was located at Met18 and Met21, the other at Met118. The $PtCl_2$ occupancies were taken as 0.75 and 0.55, respectively. The sites were consistent with those used in MIR phasing (Table 1). As to be expected, both Pt complexes were planar quadratic with the two chlorides in *trans* positions. At site 1, the other two ligands were the sulfurs of Met18 and Met21, both at a distance of 2.5 Å. At site 2, the third ligand was the sulfur of Met118 and the fourth position was occupied by a water molecule. Site 1 is at the inner side of the extracellular loop L1, whereas the quadratic complex at site 2 lies parallel to the protein surface outside the periplasmic turn T3.

A further high-resolution data set was collected with a native crystal at cryogenic temperatures, named Cryo-nat, and used in a second refinement (Table 2). A comparison of the resulting structure with that of Cryo-Pt showed some differences at the tips of the external loops L1, L2 and L3 that have the highest mobilities. Small changes also occur in the sulfur positions of the Pt-ligating methionines. The remaining structures are, within the limits of error, identical. As judged from the R factors, the mobilities and the solvent structure (Table 2), however, the quality of the native model is somewhat inferior to that of the platinum derivative. This seems to explain why the refined model of Cryo-nat fails to show clear densities

Table 1

Phasing by multiple isomorphous replacement.

	Native*	K_2PtCl_4	UO_2Ac_2
Space group	R32	R32	R32
Unit cell a = b,c (Å)	84.7, 209.6	84.5, 209.8	84.5, 209.7
Resolution range (Å)	30–3.3	30–3.7	30–3.8
Completeness (%)	99	97	88
Multiplicity	3.3	2.6	2.3
Unique reflections	4554	3093	2568
R_{sym}† (last shell) (%)	7.5 (22)	11.8 (28)	12.2 (29)
I/σ (last shell)	9.5 (3.4)	5.9 (2.6)	5.9 (2.7)
R_{iso}‡ (%)	–	22	23
Sites§	–	2	1
Phasing power#	–	1.4	1.0

*Mutant His100Asn (re)natured. All data sets were collected with Cu K_α radiation at room temperature. †$R_{sym} = \Sigma_h\Sigma_i | I_{hi} - <I_h> | / \Sigma_h\Sigma_i I_{hi}$, where h stands for the unique reflections and i counts through symmetry-related reflections. ‡$R_{iso} = \Sigma_h | I_{der} - I_{nat} | / \Sigma_h I_{nat}$, the resolution limit is 4.0 Å for K_2PtCl_4 and 4.6 Å for UO_2Ac_2. §The heavy-atom positions are: Pt site 1 (0.763, 0.002, 0.278) at Met18 and Met21; Pt site 2 (0.507, –0.173, 0.161) at Met118; UO_2 site (0.203, 0.019, 0.000) at Asp101. #Mean heavy-atom amplitude divided by the mean lack of closure.

Table 2

Data collection and refinement statistics.

	Cryo-nat	Cryo-Pt
Diffraction data set*		
Space group	R32	R32
Unit cell a = b,c (Å)	82.3, 208.1	82.4, 206.3
Resolution range	35–2.1	34–1.9
Completeness (%)	99	95
Multiplicity	3.6	3.7
Unique reflections	16,165	20,466
R_{sym} (last shell) (%)	7.6 (32)	6.1 (27)
I/σ (last shell)	11.0 (2.7)	14.6 (2.9)
Refinement and final model		
R factor (%)	23.3	20.4
R_{free} of 5% test set (%)	28.4	24.6
Average B factor (Å^2)	58	44
Rms deviations from ideality		
bonds (Å)	0.021	0.020
angles (°)	3.2	2.8
Number of nonhydrogen protein atoms	1158	1158
Water molecules	70	73
Detergent molecules	–	1
Glycerol molecules	–	2
$PtCl_2$ molecules	–	2

*Both data sets were collected at 100K at EMBL beamline X11 (DESY Hamburg) using a wavelength of 0.9057 Å. For data set Cryo-Pt, some amino acid residues were refined with two conformations: Ser3, Tyr28, Val39, Ile65, Ile79, Val83, Val85, Phe90, Thr92, Val121, Ser130 and Val144.

Figure 1

Stereoview of the Cα chain fold of OmpX. (a) View from the membrane with the external medium at the top and the periplasm at the bottom. The tips of loops L2 and L3 at the top have only poor density in the native structure (Cryo-nat), but are well defined in the platinum derivative (Cryo-Pt). (b) View from the external medium into the barrel after rotating by 90°.

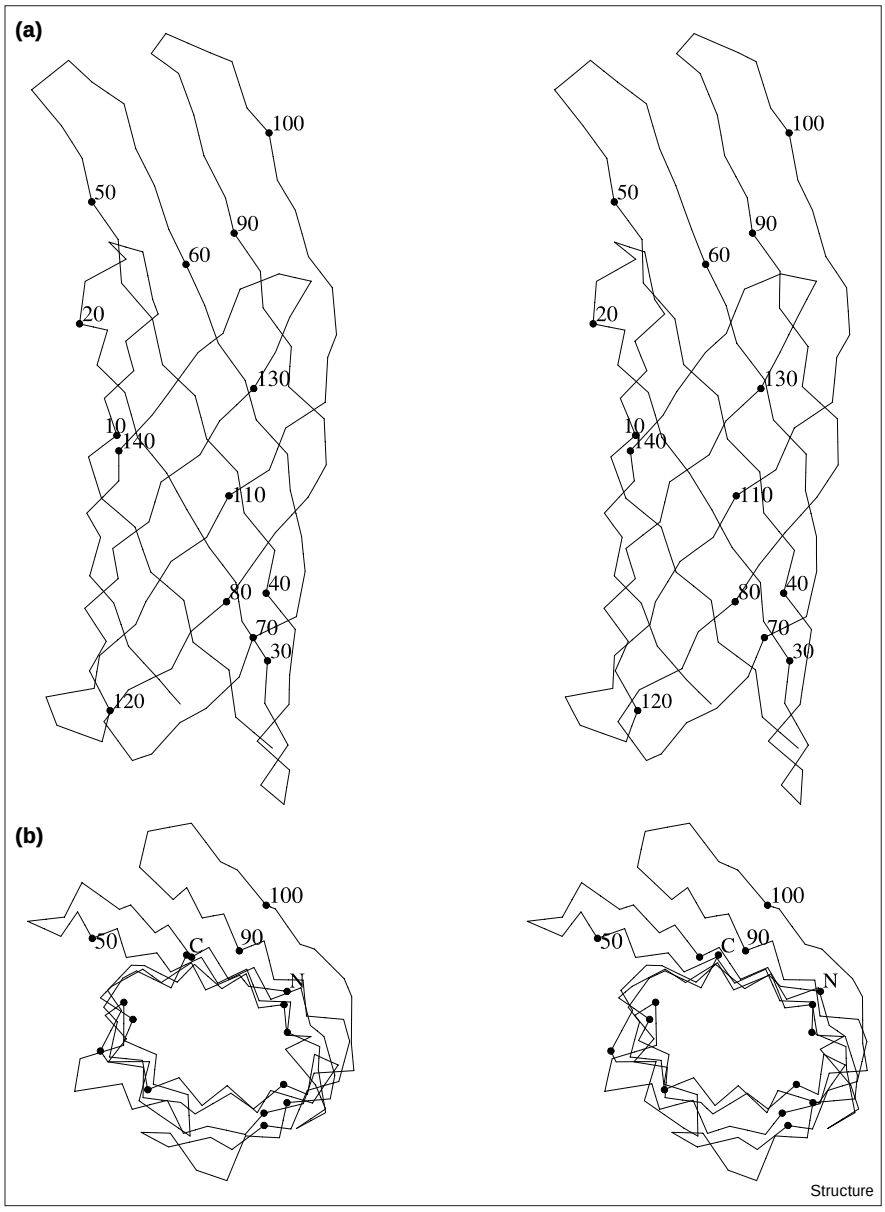

for detergent and glycerol molecules. Yet, both final models are of good quality as demonstrated by the electron density in Figure 2 and by the fact that 99% of the backbone dihedral angles are in allowed regions [15].

Description of the structure

The overall structure of OmpX is depicted in Figure 3. It contains an all-next-neighbor antiparallel eight-stranded β-barrel consisting of 122 of the 148 residues. The barrel is exceptionally long with an average strand length of 15 residues. The height of the barrel is ~32 Å, the diameter is ~20 Å. The four protruding β strands extend the protein to an overall height of ~50 Å. The Cα atom distances across the β barrel range between 10 Å and 16 Å. The cross-section of the barrel is ellipsoidal with an axes ratio of 1.6 to 1.0, as can be visualized in Figures 1b and 3.

The amino acid sequence of OmpX and the topology of the β barrel are depicted in Figure 4, which also shows the shear number (eight) of the barrel [16]. The orientation of OmpX in the membrane can be derived from experiments that identified residues exposed to the external medium [17–19]. All of these residues are at one end of the barrel (Figure 4), assigning the longer loop connections (L1, L2, L3 and L4) to the extracellular side and the shorter turn connections (T1, T2 and T3) to the periplasm. This is in

Figure 2

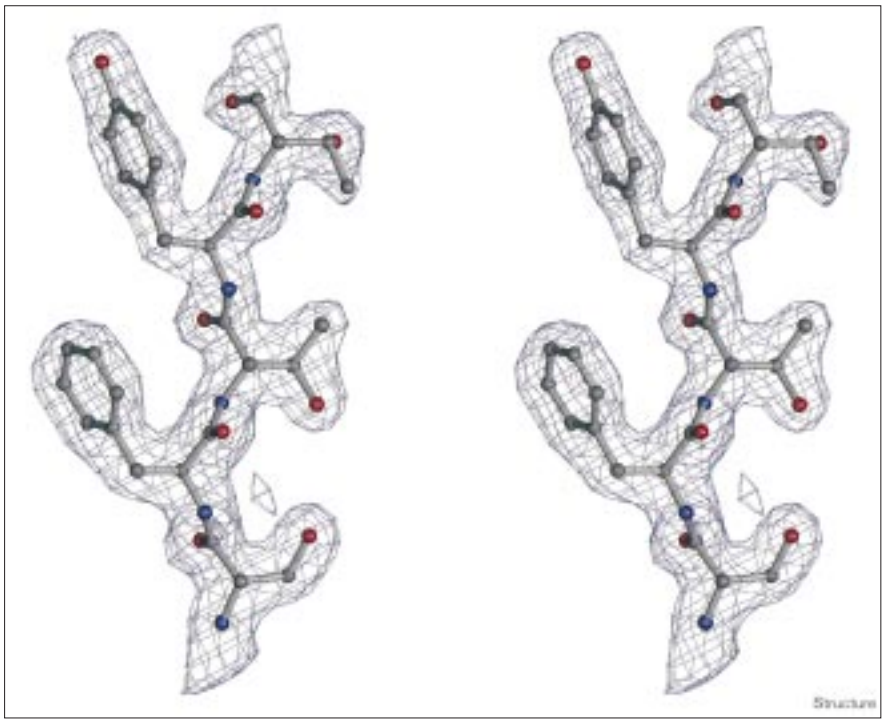

Final ($2F_o$–F_c) electron-density map at strand β3 contoured at 1.5σ for the lower quality data set Cryo-nat. Residues Phe43 and Tyr45 at the left-hand side point to the membrane moiety, whereas residues Ser42, Thr44 and Thr46 at the other side point to the barrel core.

agreement with the structures of porins [20] and also with that of OmpA [13].

In further agreement with the porins and OmpA, we show in Figure 5 that the chain mobility at loops L1 through L4 at the extracellular end of the β barrel is much higher than at the periplasmic end in turns T1, T2 and T3. A special feature of OmpX, however, is the organization of the external loops in a regular β sheet that has the appearance of a 'waving flag' (Figure 3). This β sheet is extended by hydrogen bonding across a crystallographic twofold axis in a prominent packing contact. This contact in particular was tightened by the mutation His100Asn that gave rise to analyzable crystals. We now see that the introduced asparagine forms two hydrogen bonds across the contact (Figure 3), whereas the replaced histidine was protonated at the pH of the crystallization buffer (pH 4.6), which prohibits mutual hydrogen bonding. This crucial exchange had been guided merely by the hope of allowing contact by replacing a charged sidechain with an efficient and short hydrogen-bonding residue. It turned out to be a stroke of luck.

Like other outer membrane proteins, OmpX shows two girdles of aromatic residues and a ribbon of nonpolar residues that attach to the membrane interior (Figure 3). The amino acid composition of the aromatic girdles is six phenylalanine residues, 11 tyrosines and two tryptophans; the nonpolar ribbon comprises four alanines, two isoleucines, one proline, four leucines and six valines. Altogether 12 sidechains were modeled in two alternative conformations (Table 2). Nine of them point to the membrane, whereas three (Phe90, Thr92 and Ser130) are at the inner side of the extracellular loops (Table 2).

The interior of the β barrel contains a hydrogen-bonding network that includes several charged residues. Moreover, there are eight cavities with an average size of ~34 $Å^3$, two of which lack structured water (Figure 6). With this construction OmpX resembles an inverse micelle. There is no pathway between the periplasmic and the external end of the barrel, so OmpX is very unlikely to function as a pore. The charged residues in the core are highly conserved within the protein family (Figure 7) and have low B factors of 25 to 30 $Å^2$, compared with the average B factor of 44 $Å^2$ (Table 2).

Although the protruding β sheet formed by L2 and L3 is appreciably more mobile than the remaining part of the protein (Figure 5), it is clearly defined by experimental electron density in the structure Cryo-Pt and to a lesser extent in Cryo-nat. The sheet stability is not much affected by the platinum bound at L1, because the L1 mobilities are essentially identical in both structures. Some stabilization arises from the crystal contact at Asn100, which is the only crystal contact at the extracellular portion of OmpX. This contact is likely to make L3 less mobile than L2 (Figure 5). A similar contact formed

Figure 3

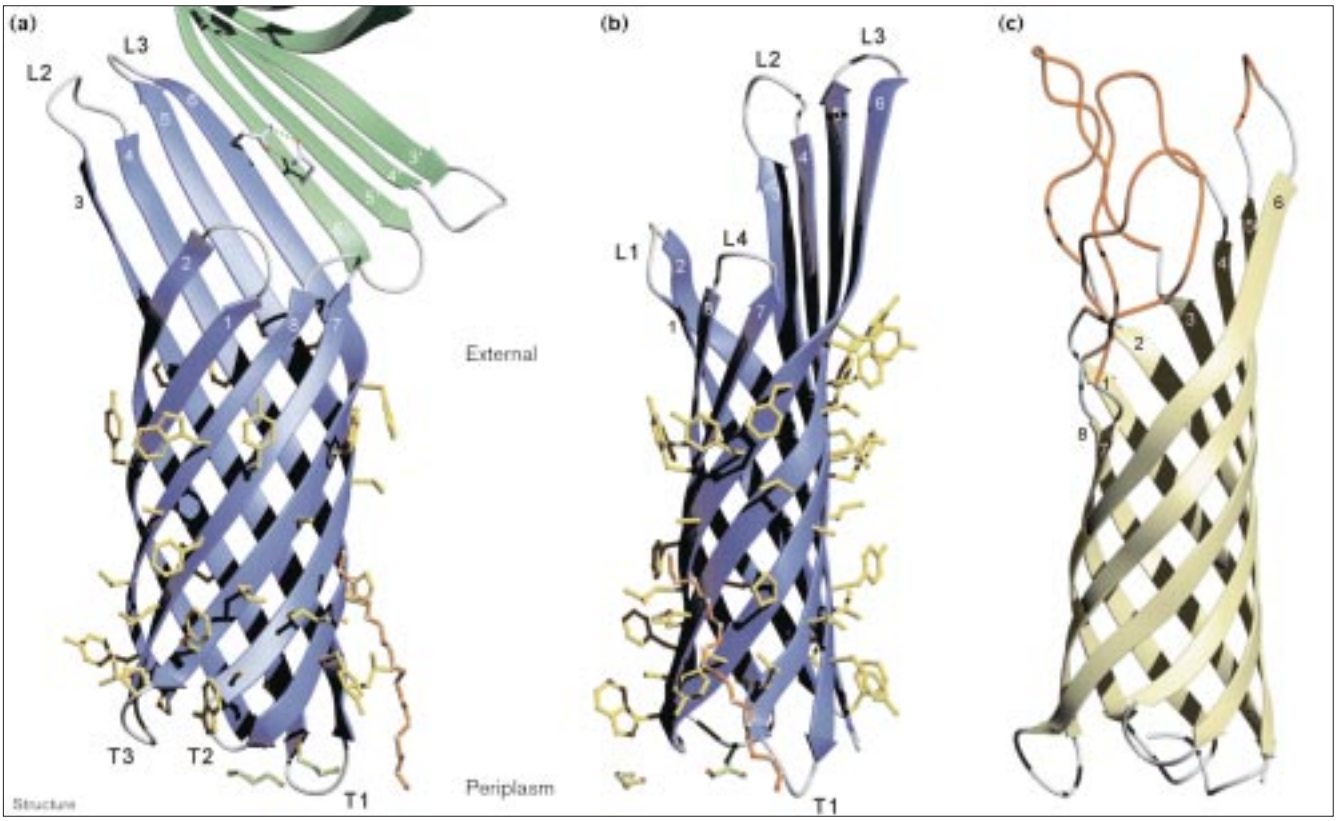

Comparisons of OmpX and the membrane domain of OmpA [13]. Ribbon plots of (a,b) OmpX (blue) and (c) OmpA (yellow). For OmpX, the residues of the aromatic girdle and the nonpolar ribbon are in yellow. The crucial crystal contact reinforced by the His100Asn mutation is shown at the top in (a). It extends the planar antiparallel β sheet to the neighboring molecule (green); Asn100 adds two hydrogen bonds. Two glycerol (green) and one C_8E_4 detergent molecule (orange) could be located; none of them is at a crystal-packing contact. OmpX is shown as viewed along the broadest projection of the β barrel in (a) and along the narrowest projection in (b). In (c) the OmpA membrane domain is shown along the narrowest projection with its mobile loops (B factor larger than 100 Å^2) colored in red.

by L3 of OmpA, however, solidified only L3 itself [13], leaving the other loops highly mobile, as indicated in Figure 3. We therefore conclude that the protruding β sheet is a structural feature of native OmpX and not a crystal artifact.

The OmpX family

OmpX shows 86% sequence identity with OmpK17 from *K. pneumoniae* and 84% identity with OmpX from *E. cloacae*. The sequence identities with Ail from *Y. enterocolitica*, PagC and Rck from *S. typhimurium* and Lom from bacteriophage λ are 45%, 39%, 38% and 30%, respectively (Figure 7). Following an earlier model of OmpA [21], Stoorvogel *et al.* [22] suggested that OmpX from *E. cloacae* consists of a similar eight-stranded β barrel with short periplasmic and longer extracellular loops. Subsequent predictions for Ail and Rck were based on the sequence homology with OmpX [17,18]. Like the OmpA model, all these models turned out to be correct within the scope of their limited information content.

Combining the sequence alignment with the structure, we now find that the homology is highest in the membrane-spanning regions and lowest in the external loops. Obviously, the membrane region forms the solid structural basis of these proteins that allows appreciable softness, that is variations, in the external loops which determine the protein's biological function. The core residues of the β barrel are the most stringently conserved ones during evolution. Here the percentage sequence identities with OmpK17, OmpX (*E. cloacae*), Ail, Rck, PagC and Lom are 100%, 100%, 71%, 69%, 67% and 55%, respectively. This conservation is also reflected in the specific sequence signature of the OmpX family Gly-X-Asn-X-Lys-Tyr-Arg-Tyr-Glu [22], which is located in strand β2 within the barrel. The asparagine and the three ionogenic residues form hydrogen bonds in the polar barrel core (Figure 6); the tyrosines are part of the aromatic girdle (Figure 4).

High variability is observed in the extracellular β strands and loops that are in contact with the environment. Several

Figure 4

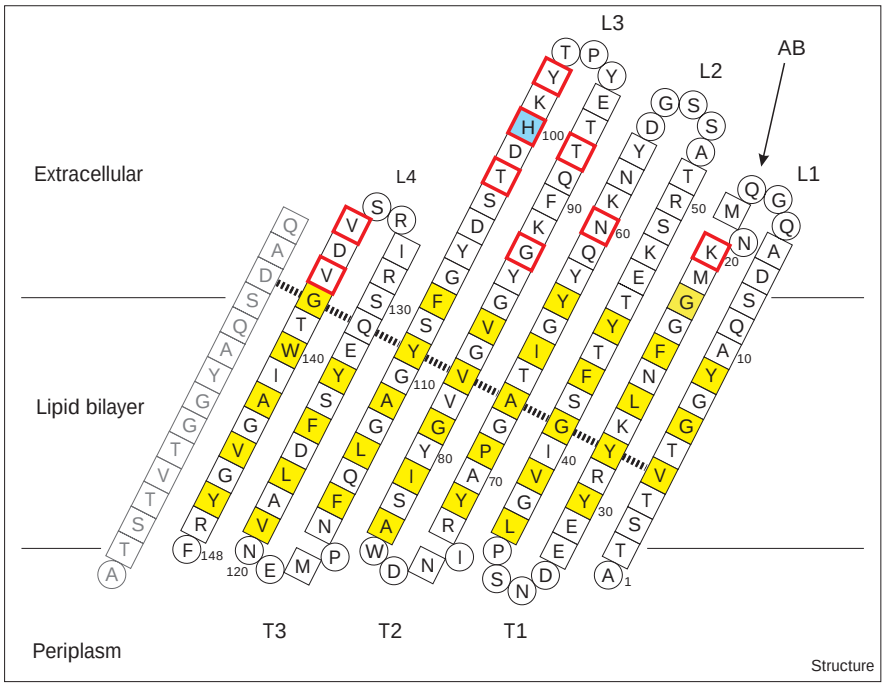

Topology plot of OmpX from *E. coli* indicating the residues pointing to the nonpolar membrane moiety (yellow). Residues in β strands are shown in squares; other residues are in circles. The first strand is given twice to clarify the circular connection. The barrel shear number is eight. An external antibody-binding site (AB) of OmpX is indicated by an arrow. Residue positions involved in virulence and defense of Rck of *S. typhimurium* (Lys20 and Thr88) and of Ail of *Y. enterocolitica* (Asn60, Gly92, Tyr98, His100, Thr102, Val135 and Val137) are marked in red. They were assigned to the OmpX sequence according to the alignment in Figure 7. The packing contact mutation His100Asn is marked in blue. The dashed black line indicates the hydrogen-bonding register within the β barrel.

experiments indicated that the extracellular loop L3 has the most important role in cell invasion and serum resistance, and thus in virulence (Figure 4). These observations now find a structural explanation. The peculiar waving flag structure of the protruding β sheet formed by L2 and L3 is likely to function as a 'fishing rod' (Figure 3), presenting the edge of the β sheet at L3 as an efficient hydrogen bonding partner. This edge is a general binding feature because it fits the edges of other β sheets as they occur, for instance, at the surface of many proteins with central parallel β sheets covered on both sides by α helices. We therefore suggest that this β-sheet edge functions in cell adhesion and invasion and that it inhibits the complement system by binding one of its essential proteins.

Figure 5

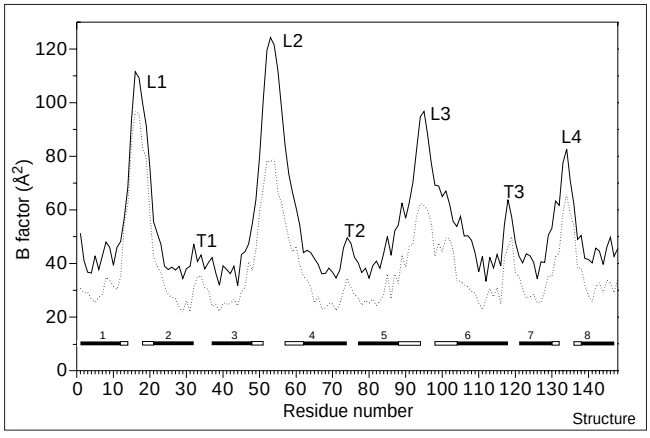

B factors of the Cα atoms of OmpX when refined against the data set Cryo-nat (solid line) and against data set Cryo-Pt (broken line). The β strands are indicated by bars that are black within the membrane-spanning part and white outside this region. The external loops (L) and the periplasmic turns (T) are labeled. The average B factors are 58 Å² and 44 Å² for the Cryo-nat and Cryo-Pt structures, respectively.

It is worth mentioning that the defined structure of a protruding single-layer β sheet is exceptional. In all other known outer membrane protein structures, and in particular in OmpA, there is no such β sheet and the external loops are much more mobile, prohibiting a tight attachment to an external protein. Interestingly, the OmpX β-sheet edge demonstrated its binding abilities by forming an important contact in our crystal packing.

Alignment with other membrane proteins

The structures of OmpX and OmpA should be related to other outer membrane proteins that have been predicted to consist of eight-stranded β barrels [23]. In the proposed alignment, the whole structural family has several features in common, like the invariant length of turn T3 which we observe as a tight turn that had been precisely predicted. Moreover, the authors that made this earlier prediction also pointed to several conserved glycine residues at barrel positions where a sidechain would protrude into the barrel interior. In OmpX, these glycines are at positions 8, 23, 38, 84, 88, 106, 110, 112, 143 and 145, most of which are at the outer edges of the elliptical barrel cross-section, forming

Figure 6

Hydrogen-bonding network (dashed lines) inside the β barrel. All residues pointing into the barrel core and all water molecules in the core (green) are shown. Two water-free internal cavities are shown in blue.

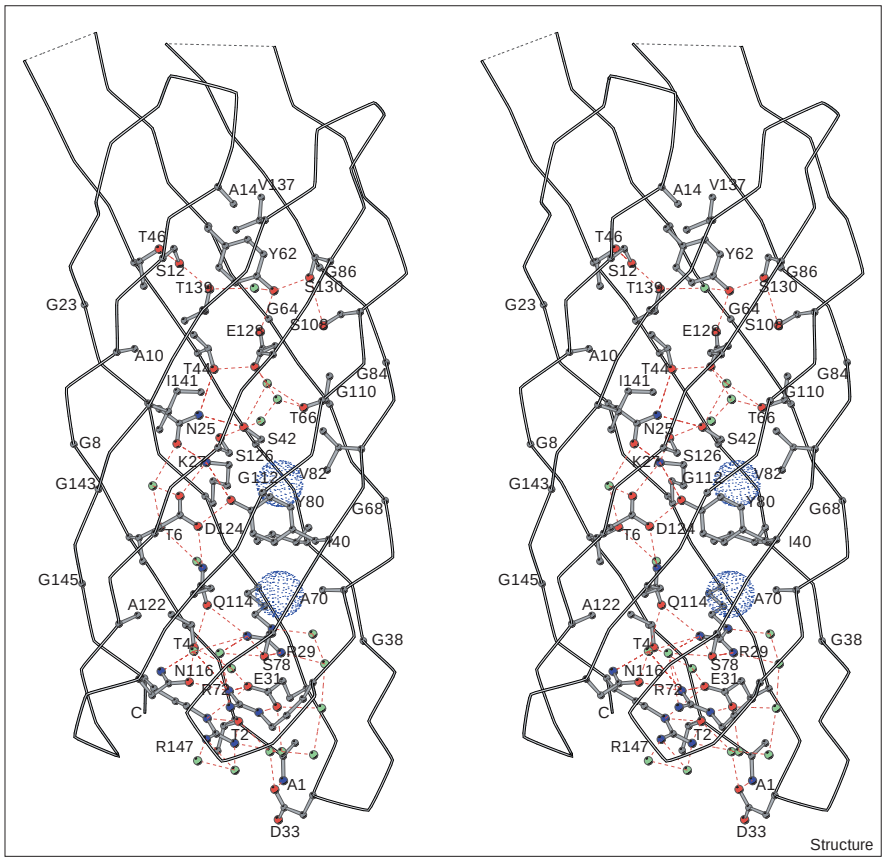

sharp bends. Their backbone dihedral angles are at the borderline between those allowed for residues with and without sidechains [15].

A comparison between OmpX and OmpA shows that their β barrels have different shear numbers, eight for OmpX and ten for OmpA. As a consequence, the average tilt of the β strands of OmpX against the barrel axis is 35° which is 7° smaller than the 42° tilt of OmpA. This 7° difference agrees with a rough estimate based on the β-sheet topology of Figure 4. The shear number difference is probably related to the more ellipsoidal cross-section of OmpX (ratio 1.6 to 1.0) compared with that of OmpA, with a ratio of 1.2 to 1.0. Moreover, the cross-sectional area of OmpX

Figure 7

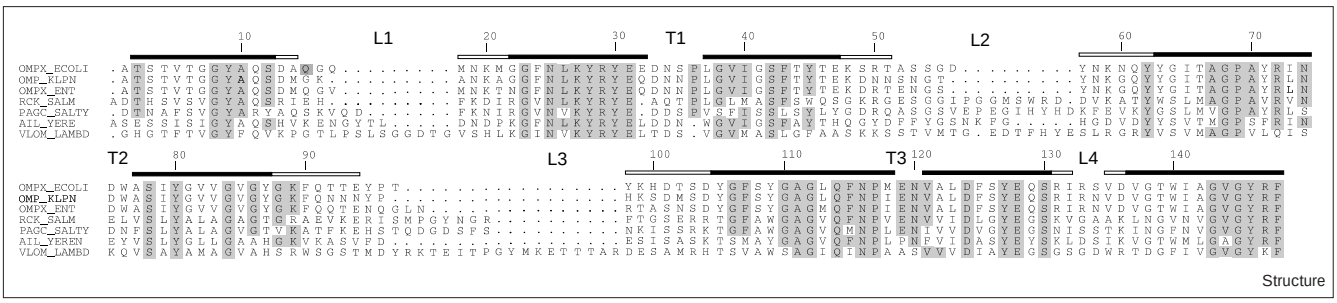

Alignment of OmpX and the six outer membrane proteins that can be related by sequence homology. The numbering is for the structure of OmpX from *E. coli* presented here (top line). Loops (L) and turns (T) are labeled. Shaded residues are conserved. β Strands are represented as black bars within the membrane-spanning part of the barrel and white bars outside. From top to bottom the proteins are OmpX from *E. coli*, OmpK17 from *K. pneumoniae*, OmpX from *E. cloacae*, Rck and PagC from *S. typhimurium*, Ail from *Y. enterocolitica* and Lom from bacteriophage λ.

is only 80% of that of OmpA, indicating that the shear number may be correlated with the volume of the sidechains buried inside the β barrel. The root mean square (rms) deviation of the Cα atoms of the OmpX and OmpA β barrels amounts to 3.3 Å for the 102 amino acid residues in the membrane-spanning regions. This explains our failure to solve the OmpX structure by the molecular replacement method using OmpA. Furthermore, the hydrogen-bonding network in the barrel core differs appreciably in these two proteins.

Apart from the OmpX and OmpA families, other outer membrane proteins are predicted to form eight-stranded antiparallel β barrels. Among these are Omp21 from *Comamonas acidovorans*, the Opa proteins from Neisseriaceae and PorF from *Pseudomonas aeruginosa* [23]. All are probably structurally related to OmpX or OmpA. A common feature of all bacterial outer membrane proteins is the C-terminal consensus sequence X-Z-X-Z-X-Z-X-Tyr-X-Phe (where X is any amino acid and Z is a nonpolar residue) [22]. This sequence may be important for protein folding and insertion into the outer membrane.

Biological implications

Bacteria have developed numerous strategies for neutralizing host defense mechanisms. One such mechanism is related to a family of 17–19 kDa outer membrane proteins found in Enterobacteriacae and bacteriophage λ. These proteins are highly conserved among pathogenic and non-pathogenic bacteria. OmpX from *Escherichia coli* belongs to this family and its structure is presented here. The protein forms an eight-stranded antiparallel β barrel of ellipsoidal cross-section, with a peculiar single-layer four-stranded β sheet protruding into the extracellular medium. We suggest that the exposed β-sheet edge functions as a 'fishing rod' that binds to numerous external proteins which have a complementary β strand at their surface, like many α/β proteins. We also suggest that this general binding affinity is used to achieve cell adhesion and invasion and to interfere with the human complement defense system, thus causing virulence.

Materials and methods

Protein purification and crystallization

The His100Asn mutant of OmpX from *E. coli* was purified and crystallized as described [12]. Briefly, the *ompX* gene was amplified from genomic *E. coli* DNA using polymerase chain reaction (PCR) techniques. It was cloned into the *Nde* I-digested expression vector pET-3b (Novagen). Mutagenesis was carried out using the Sculptor Kit (Amersham) after subcloning into the vector M13mp19 (Boehringer Mannheim). OmpX was expressed in *E. coli* strain BL21(DE3)pLysS (Novagen) without the periplasmic signal sequence and thus into inclusion bodies.

After cell lysis and several washing steps, the inclusion bodies were solubilized in 6 M guanidinium hydrochloride in buffer P (20 mM Tris-HCl pH 8.5) and refolded by subsequent dilution with buffer P containing 5% (w/v) n-octylpolyoxyethylene (C_8POE, Bachem) with 0.6 M L-arginine. We observed that native OmpX runs faster in sodium dodecyl sulfate (SDS) gels if the sample had been heated to 100°C for 10 min beforehand. The same behavior is known for OmpA [13]. As a consequence, the refolding to the native conformation could be monitored by SDS–PAGE (polyacrylamide gel electrophoresis). The protein solution was dialyzed twice for 24 h against 1 L buffer P with 1% (w/v) C_8POE, loaded on a Source-Q ion exchange column (Pharmacia) equilibrated with buffer P with 0.6% (w/v) C_8E_4 and washed with the same buffer. OmpX did not bind to the column material. Analysis of the flowthrough by SDS–PAGE, electrospray mass spectrometry and N-terminal sequencing showed that the protein solution was pure and that the N-terminal methionine, which replaced the signal sequence, was cleaved off completely.

Crystals were grown at room temperature by hanging-drop vapor diffusion against a reservoir solution of 30% (v/v) 2-propanol, 20% (v/v) glycerol, 0.2 M $CaCl_2$ and 0.1 M sodium acetate pH 4.6. The isoelectric point calculated from the sequence is 5.0. The crystallization drops contained equal volumes (2 μl) of reservoir solution and purified OmpX (20 mg/ml in buffer P with 0.6% (v/v) C_8E_4). The crystals grew up to sizes around $300 \times 200 \times 200$ μm^3 and diffracted X-rays isotropically to beyond 1.9 Å resolution. They contained one monomer (M_r 16,360 for mutant His100Asn) per asymmetric unit. The solvent content of the crystals was 70% corresponding to a V_M of 4.1 Å^3/Da, which is a common value for membrane proteins.

Data collection

Crystals were either mounted in capillaries and kept at 20°C during data collection or flash-frozen to 100K. Crystals could be frozen directly from the crystallization buffer by flipping them into the cryo stream. Data were collected on a MAR300 image-plate detector using a 0.3 mm diameter collimated Cu K_α radiation from a rotating-anode generator (Rigaku, model RU2HC) at 45 kV and 120 mA. Synchrotron data were collected at 100K on EMBL beamline X11 at DESY (Hamburg) with a MAR345 image plate. All diffraction data were processed using the programs MOSFLM, SCALA and TRUNCATE [14].

Heavy-atom derivatives and phasing

The structure was solved by MIR. The platinum and uranyl derivatives were obtained by soaking the crystal for 1 h in 20 μl reservoir solution containing 20 mM K_2PtCl_4 or 10 mM UO_2Ac_2, respectively. Derivative data and the corresponding native data were measured at room temperature (Table 1) and scaled using the program SCALEIT [14]. The heavy-atom positions of both derivatives were determined from inspection of the difference-Patterson maps and confirmed by using difference-Fourier methods. The positions were refined using MLPHARE [14] and protein phases were determined to 4.5 Å resolution, resulting in an overall figure of merit of 0.48 (all reflections). Several rounds of solvent flattening and phase extension using the program DM [14] followed. The electron-density map calculated from these phases at 3.3 Å resolution was readily interpretable.

Model building and refinement

A model of the protein was first built as a polyalanine chain into clear electron-density regions using the program O [24]. Most of the sidechains could be identified from the known sequence. The initial model contained 128 amino acids. After several cycles of refinement using REFMAC [14], we changed to data set Cryo-Pt and run through a rigid-body refinement using the program X-PLOR [25]. All 148 residues were built into the model by concomitant inspection of the $(2F_o–F_c)$ and the $(F_o–F_c)$ difference electron-density maps. The resulting model was then refined using REFMAC. Subsequently, the model was refined against data set Cryo-nat, starting with a simulated annealing protocol in the program X-PLOR. The refinement was continued with the program REFMAC. In both structures, the water molecules were first placed using the program ARPP [14] and then included into REFMAC. The internal cavities were calculated with a probe radius of 1.4 Å using the program MSP [26]. For figure production the programs MOLSCRIPT [27], RASTER3D [28] and MOLMOL [29] were used.

Accession numbers

The atomic coordinates and the structure factors have been deposited in the Protein Data Bank with the accession codes 1QJ8 and 1QJ9, respectively.

Acknowledgements

We thank the team of the EMBL outstation Hamburg for help with synchrotron data collection, T Hoffmann for providing us with genomic *E. coli* DNA, P Hörth and W Haehnel for ESI-MS measurements and C Vonrhein for computational help. The project was supported by the Deutsche Forschungsgemeinschaft under SFB-428 and by the European HCM Network CT940690.

References

1. Heffernan, E.J., Wu, L., Louie, J., Okamoto, S., Fierer, J. & Guiney, D.G. (1994). Specificity of the complement resistance and cell association phenotypes encoded by the outer membrane protein genes *rck* from *Salmonella typhimurium* and *ail* from *Yersinia enterocolitica*. *Infect. Immun.* **62**, 5183-5186.
2. Mecsas, J., Welch, R., Erickson, J.W. & Gross, C.A. (1995). Identification and characterization of an outer membrane protein, OmpX, in *Escherichia coli* that is homologous to a family of outer membrane proteins including Ail of *Yersinia enterocolitica*. *J. Bacteriol*. **177**, 799-804.
3. de Kort, G., Bolton, A., Martin, G., Stephen, J. & van de Klundert, J.A.M. (1994). Invasion of rabbit ileal tissue by *Enterobacter cloacae* varies with the concentration of OmpX in the outer membrane. *Infect. Immun*. **62**, 4722-4726.
4. Stoorvogel, J., van Bussel, M.J.A.W.M. & van de Klundert, J.A.M. (1987). Cloning of a β-lactam resistance determinant of *Enterobacter cloacae* affecting outer membrane proteins of *Enterobacteriaceae*. *FEMS Microbiol. Lett.* **48**, 277-281.
5. Climent, N., Ferrer, S., Rubires, X., Merino, S., Tomás, J.M. & Regué, M. (1997). Molecular characterization of a 17-kDa outer-membrane protein from *Klebsiella pneumoniae*. *Res. Microbiol.* **148**, 133-143.
6. Pulkkinen, W.S. & Miller, S.I. (1991). A *Salmonella typhimurium* virulence protein is similar to a *Yersinia enterocolitica* invasion protein and a bacteriophage lambda outer membrane protein. *J. Bacteriol.* **173**, 86-93.
7. Heffernan, E.J., Reed, S., Hackett, J., Fierer, J., Roudier, C. & Guiney, D. (1992). Mechanism of resistance to complement-mediated killing of bacteria encoded by the *Salmonella typhimurium* virulence plasmid gene *rck*. *J. Clin. Invest.* **90**, 953-964.
8. Miller, V.L., Bliska, J.B. & Falkow, S. (1990). Nucleotide sequence of the *Yersinia enterocolitica ail* gene and characterization of the Ail protein product. *J. Bacteriol.* **172**, 1062-1069.
9. Bliska, J.B. & Falkow, S. (1992). Bacterial resistance to complement killing mediated by the Ail protein of *Yersinia enterocolitica*. *Proc. Natl Acad. Sci. USA* **89**, 3561-3565.
10. Barondess, J.J. & Beckwith, J. (1990). A bacterial virulence determinant encoded by lysogenic coliphage λ. *Nature* **346**, 871-874.
11. Pacheco, S.V., González, O.G. & Contreras, G.L.P. (1997). The *lom* gene of bacteriophage λ is involved in *Escherichia coli* K12 adhesion to human buccal epithelial cells. *FEMS Microbiol. Lett.* **156**, 129-132.
12. Pautsch, A., Vogt, J., Model, K., Siebold, C. & Schulz, G.E. (1999). Strategy for membrane protein crystallization exemplified with OmpA and OmpX. *Proteins* **34**, 167-172.
13. Pautsch, A. & Schulz, G.E. (1998). Structure of the outer membrane protein A transmembrane domain. *Nat. Struct. Biol*. **5**, 1013-1017.
14. Collaborative Computational Project Number 4 (1994). The CCP4 Suite: programs for protein crystallography. *Acta Crystallogr. D* **50**, 760-763.
15. Laskowski, R.A., MacArthur, M.W., Moss, D.S. & Thornton, J.M. (1993). PROCHECK: a program to check the stereochemical quality of protein structures. *J. Appl. Crystallogr.* **26**, 283-291.
16. Liu, W.-M. (1998). Shear numbers of protein β-barrels: definition refinements and statistics. *J. Mol. Biol.* **275**, 541-545.
17. Beer, K.B. & Miller, V.L. (1992). Amino acid substitutions in naturally occurring variants of Ail result in altered invasion activity. *J. Bacteriol.* **174**, 1360-1369.
18. Cirillo, D.M., Heffernan, E.J., Wu, L., Harwood, J., Fierer, J. & Guiney, D.G. (1996). Identification of a domain in Rck, a product of the *Salmonella typhimurium* virulence plasmid, required for both serum resistance and cell invasion. *Infect. Immun.* **64**, 2019-2023.
19. de Kort, G., van der Bent-Klootwijk, P. & van de Klundert, J.A.M. (1998). Immuno-detection of the virulence determinant OmpX at the cell surface of *Enterobacter cloacae*. *FEMS Microbiol. Lett.* **158**, 115-120.
20. Schulz, G.E. (1996). Porins: general to specific, native to engineered passive pores. *Curr. Opin. Struct. Biol.* **6**, 485-490.
21. Vogel, H. & Jähnig, F. (1986). Models of the structure of outer membrane proteins of *Escherichia coli* derived from Raman spectroscopy and prediction methods. *J. Mol. Biol.* **190**, 191-199.
22. Stoorvogel, J., van Bussel, M.J.A.W.M., Tommassen, J. & van de Klundert, J.A.M. (1991). Molecular characterization of an *Enterobacter cloacae* outer membrane protein (OmpX). *J. Bacteriol*. **173**, 156-160.
23. Baldermann, C., Lupas, A., Lubieniecki, J. & Engelhardt, H. (1998). The regulated outer membrane protein Omp21 from *Comamonas acidovorans* is identified as a member of a new family of eight-stranded β-sheet proteins by its sequence and properties. *J. Bacteriol.* **180**, 3741-3749.
24. Jones, T.A., Zou, J.Y., Cowan, S.W. & Kjelgaard, M. (1991). Improved methods for building protein models in electron density maps and the location of errors in these models. *Acta Crystallogr. A* **47**, 110-119.
25. Brünger, A.T. (1993). *X-PLOR Version 3.1: A System for X-ray Crystallography and NMR*. Yale University Press, New Haven.
26. Connolly, M.L. (1993). The molecular surface package. *J. Mol. Graph*. **11**, 139-141.
27. Kraulis, P.J. (1991). MOLSCRIPT – a program to produce both detailed and schematic plots of protein structures. *J. Appl. Crystallogr*. **24**, 946-950.
28. Merritt, E.A. & Bacon, D.J. (1997). Raster3D: photorealistic molecular graphics. *Methods Enzymol.* **277**, 505-524.
29. Koradi, R., Billeter, M. & Wüthrich, K. (1996). MOLMOL: a program for display and analysis of macromolecular structures. *J. Mol. Graph.* **14**, 51-55.